Research article

X-RAY SPECTROMETRY

Received: 29 July 2014 Revised: 22 January 2015 Accepted: 22 January 2015 Published online in Wiley Online Library

(wileyonlinelibrary.com) DOI 10.1002/xrs.2602

Identification of local and allochthonous flint artefacts from the Middle Palaeolithical site 'Abrigo de la Quebrada' (Chelva, Valencia, Spain) by macroscopic and physicochemical methods†

Clodoaldo Roldán,[a]* Jorgelina Carballo,[a] Sonia Murcia,[a] Aleix Eixea,[b] Valentín Villaverde[b] and João Zilhão[c]

This work summarizes the characterization of flint artefacts from the Middle Palaeolithic site 'Abrigo de la Quebrada' (Chelva, Valencia, Spain) and flint geological samples collected in the Chelva area. Additionally, some flint artefacts located outside this geographical zone were also analysed and compared with the samples from the Abrigo de la Quebrada site. Flint samples have been studied using methods of macroscopic description and physicochemical analysis [energy dispersive X-ray fluorescence spectrometry (EDXRF) and X-ray diffraction (XRD)]. Multivariate statistical analysis of the EDXRF data and the determination of the crystalline index of quartz, obtained from the XRD patterns, are suitable methods to discriminate between local and allochthonous flint artefacts in agreement with the macroscopic classification. These results provide new analytical information of the flint artefacts on a geographical area that had not been studied so far. Copyright © 2015 John Wiley & Sons, Ltd.

Introduction

Flint is a lithic material that can be worked to obtain sharp blades with conchoidal fractures characteristic of lithic tools as scrapers, hand axes and arrowheads. These artefacts represent the majority of the lithic material from the Palaeolithic sites worldwide, and it continued to be used during subsequent periods to manufacture some of the earliest tools used by man. One of the questions that archaeologists are keen to answer in relation to flint use and characterization is sourcing. Answering this question is important to reconstruct interaction networks of prehistoric cultures. Over the past years, a great variety of analytical methods have been applied to identify the sources of flint artefacts found in different archaeological contexts.[1–8] The objective of these studies is to determine the chemical composition of geological and archaeological flint samples and to obtain element correspondences to establish the probable geological source of origin for archaeological artefacts.

Despite the great interest in sourcing of flint and lithic technology, the information available for the Valencian Community (East Spain) on prehistoric raw material sources and their analytical characterization is scant. Some studies have been carried out over limited areas only, and geological mapping of the distribution of the siliceous variants used is nonexistent. The available data pertain mostly to the southern region of the Valencian Community.[9–12] As far as the central region of the Valencian Community (province of Valencia) is concerned, no systematic work has been done to characterize the geochemical composition of flint samples from archaeological sites. In this region, the research has been limited to isolated classification of finds from the sites of Parpalló[13] (Gandía, Valencia, Spain) and Cova Negra[14] (Xátiva, Valencia, Spain) deposited in museum collections. This lack of information is significant in the Middle Palaeolithic period and limits attempts at establishing a framework for the discussion of patterns of human mobility during this period. Recently, raw flint materials found at the Abrigo de la Quebrada site (Chelva, Valencia, Spain) have been classified according to macroscopic features and have allowed some interesting insights.[15]

The aim of this paper is to compare the application of physicochemical [energy dispersive X-ray fluorescence spectrometry (EDXRF) and X-ray diffraction (XRD)] and macroscopic methods to lithic artefacts studies with the purpose of evaluating the potential of these techniques to discriminate between local and allochthonous raw materials and show how, in our case, the complementarity of the two methods was useful for the study of flint from the Abrigo de la Quebrada site and the surrounding area.

Material and methods

The Abrigo de la Quebrada rock shelter is located in Chelva, some 65 km NW of the city of Valencia (Fig. 1). The rock shelter is 38 m long, between 2 and 9 m deep and part of the Iberian

* *Correspondence to: Clodoaldo Roldán, Instituto de Ciencia de los Materiales, Universidad de Valencia (ICMUV), C/ Catedrático José Beltrán, 2, 46980 Paterna, Valencia, Spain. E-mail: clodoaldo.roldan@uv.es*

† *Presented at the European Conference on X-Ray Spectrometry, Bologna, Italy, 15-20 June 2014*

a *Instituto de Ciencia de los Materiales, Universidad de Valencia (ICMUV), C/ Catedrático José Beltrán, 2, 46980, Paterna, Valencia, Spain*

b *Departamento de Prehistoria y Arqueología, Universidad de Valencia, Av. Blasco Ibáñez, 28, 46010, Valencia, Spain*

c *ICREA – Departament de Prehistòria, Història Antiga i Arqueologia, Universitat de Barcelona/ICREA, C/ Montalegre 6, 08001, Barcelona, Spain*

Copyright © 2015 John Wiley & Sons, Ltd.

Figure 1. Map with the localization of the Abrigo de la Quebrada site.

Range(Cordillera Ibérica) geological unit, which belongs to the Kimmeridgian Stage in the Upper Jurassic Series, which occurred between 157.3 and 152.1 millions of years ago during the Jurassic Period (ca. 201–145 millions of years ago) and features the deposition of pisolitic and oolitic limestone (sedimentary rocks composed of calcium carbonate, phosphate, chert or iron minerals, formed from concretionary spherical grains disposed on concentric layers named pisolites, if their diameter is higher than 2 mm, or oolites, if their diameter is lower than 2 mm) in a neritic to coastal shallow marine environment that corresponds to the continental shelf with depths of 30 to 40 m. The stratigraphy features a total of eight units and a thickness of some 3 m. Only levels II through V, VII and VIII show evidence of human occupation. Accelerator mass spectrometry (AMS) dating, undertaken on the remaining charcoals, gave a radiocarbon determination of 40 500 ± 530 BP for level III and 43 930 ± 750 BP and >50 800 BP for level IV.[15]

The analysis of most of the samples included in this work was conditioned to the use of non-destructive techniques. As valuable specimens, it was unacceptable to obtain petrographic thin sections of the material or subject it to destructive analytical techniques. In this sense and in our case, destructive analysis of the archaeological flint artefacts was not an option. Certainly, other options can offer more sensitive analyses but by means of destructive protocols. Therefore, in this work, flint samples have been studied using macroscopic description methods (by means of a stereomicroscope) and non-destructive analyses by means of portable EDXRF instrumentation, directly on the untreated samples. We have considered these techniques as the best option based on instruments accessibility and current moral and legal constraints. Only a limited number of the flint artefacts were available for destructive analysis, and we considered the option of XRD analysis to obtain the crystallinity index (IC) of quartz in order to test their effectiveness to identify local and allochthonous flint artefacts. These techniques have shown their feasibility to discriminate between local and allochthonous samples.

Selected samples

Forty-one flint artefacts from the archaeological site of Abrigo de la Quebrada (sample codes D and A in Table 1), five samples quarry out from the Chelva regional outcrops (sample code M in Table 1) and nine foreign samples – four flint artefacts from the archaeological site of 'Cova de les Cendres' (Moraira, Alicante; sample code CC in Table 1), two flint artefacts from the archaeological site of 'Cova Negra' (Xátiva, Valencia; sample code CN in Table 1) and three samples from natural flint outcrops located outside the geographical zone of Chelva (sample code UV in Table 1) – were characterized and classified according to macroscopic features. Macroscopic analysis of these samples was carried out with a stereomicroscope under 40× magnification and used Munsell and Pantone tables for recording texture, impurities, fossil presence, cortex features and colour. All these samples were also analysed in non-destructive mode by means of EDXRF spectrometry. A selected set of the samples (21 flint artefacts and five geological samples) were analysed by XRD spectrometry, and crystalline phases and IC of quartz were obtained. Foreign samples were compared with the samples from the Abrigo de la Quebrada site for the assessment of the provenance of the site's allochthonous flints.

EDXRF analyses

In an attempt to find a reliable methodology for chemically characterizing flint materials, the samples were analysed by means of a portable EDXRF spectrometer with an X-ray tube (40 kV/50 μA, maximum) with a silver anode operating in transmission mode.[16] The spectrometer has a thermoelectrically cooled Si-PIN detector which has an active area of 6 mm^2 and 12.5 μm beryllium window. The X-ray beam is collimated by an aluminium collimator, and the

Table 1. Analysed flint samples (see text for details)

Sample code	# of samples	Range	Site	Origin
D	14	D8 → D20	Abrigo de la Quebrada (Chelva, Valencia)	archaeological
A1	5	A1-3 → A1-7	Abrigo de la Quebrada	archaeological
A2	9	A2-11 → A2-19	Abrigo de la Quebrada	archaeological
A3	8	A3-7 → A3-14	Abrigo de la Quebrada	archaeological
A4	5	A4-1 → A4-5	Abrigo de la Quebrada	archaeological
M	5	M6 →M10	Chelva quarries	geological
CN	2	CN-1 → CN-2	Cova Negra (Xátiva, Valencia)	archaeological
CC	4	CC3-1 → CC3-4	Cova Cendres (Moraira Alicante)	archaeological
UV1	1		Penella quarries (Alicante)	geological
UV2	1		Beniaia quarries (Alicante)	geological
UV3	1		Mora de Rubielos quarries (Teruel)	geological

Copyright © 2015 John Wiley & Sons, Ltd.

Table 2. Normalized net areas from the elements detected by EDXRF

SAMPLE	Si	P	S	Cl	K	Ca	Ti	V	Fe	Cu	Zn	Sr
D8	4.14E-02	6.45E-05	1.00E-04	7.89E-04	1.43E-03	7.75E-03	9.38E-04	2.63E-03	2.63E-02	6.64E-04	4.85E-03	2.35E-03
D9	3.47E-02	1.37E-04	1.73E-04	4.49E-04	8.66E-04	6.74E-03	6.82E-04	3.47E-03	3.41E-02	1.41E-03	4.77E-03	2.14E-03
D10	3.30E-02	1.06E-04	1.34E-04	6.64E-04	2.41E-03	3.53E-03	1.31E-03	3.41E-03	3.88E-02	9.21E-04	3.79E-03	1.63E-03
D11	3.01E-02	1.92E-04	8.97E-06	2.06E-03	1.30E-03	8.43E-02	5.59E-04	2.04E-03	2.78E-02	3.69E-06	4.20E-03	2.20E-03
D12	3.74E-02	1.33E-04	2.06E-04	8.80E-04	1.88E-03	3.12E-03	8.22E-04	4.13E-03	3.93E-02	4.76E-04	3.99E-03	2.49E-03
D13	3.62E-02	1.22E-04	9.33E-05	8.79E-04	1.24E-03	1.97E-03	2.13E-04	2.26E-03	1.92E-02	5.46E-04	4.20E-03	2.40E-03
D14	3.46E-02	5.43E-05	1.06E-04	6.65E-04	2.45E-03	3.19E-02	8.74E-04	2.95E-03	4.74E-02	6.13E-05	3.61E-03	2.00E-03
D15	3.86E-02	1.26E-04	5.55E-05	1.02E-03	2.35E-03	2.60E-03	1.29E-03	2.90E-03	3.42E-02	7.68E-04	5.90E-03	1.35E-03
D16	3.76E-02	2.67E-04	7.09E-05	5.98E-04	3.79E-03	3.03E-02	1.32E-03	2.70E-03	5.27E-02	1.00E-04	4.80E-03	3.72E-03
D17	3.62E-02	4.20E-05	1.79E-04	1.04E-04	2.66E-03	3.07E-03	1.20E-03	3.40E-03	4.30E-02	9.96E-04	3.53E-03	2.37E-03
D18	3.77E-02	3.97E-05	2.34E-04	4.19E-04	1.91E-03	2.44E-03	1.05E-03	3.33E-03	3.36E-02	2.82E-04	4.59E-03	2.09E-03
D19	3.71E-02	1.73E-04	8.00E-06	8.92E-04	2.02E-03	3.13E-03	1.14E-03	3.06E-03	3.49E-02	8.63E-04	3.94E-03	2.50E-03
D20	3.62E-02	1.43E-04	2.75E-04	1.18E-03	3.34E-03	1.15E-02	4.09E-04	2.67E-03	1.67E-02	4.49E-04	3.82E-03	7.69E-03
A1-3	3.82E-02	1.23E-04	4.71E-05	1.46E-04	8.16E-06	4.40E-04	4.00E-05	3.22E-03	9.70E-03	3.81E-04	3.19E-03	9.81E-04
A1-4	3.58E-02	4.15E-05	1.57E-04	6.76E-05	3.87E-04	1.46E-02	6.25E-05	2.67E-03	1.23E-02	8.77E-04	3.33E-03	2.12E-04
A1-5	4.12E-02	4.12E-05	5.45E-05	9.04E-05	2.31E-04	1.01E-03	3.94E-04	3.56E-03	1.19E-02	8.06E-04	4.56E-03	1.57E-04
A1-6	3.79E-02	1.84E-04	9.20E-05	2.22E-04	6.61E-04	1.49E-02	1.00E-04	3.03E-03	1.34E-02	2.97E-04	4.18E-03	9.07E-04
A1-7	3.84E-02	6.20E-05	8.06E-05	2.04E-04	1.04E-03	2.11E-04	2.36E-04	3.19E-03	1.36E-02	5.26E-04	4.41E-03	1.50E-03
A2-11	3.80E-02	1.88E-04	1.43E-05	3.40E-05	1.12E-04	5.62E-05	2.37E-04	2.74E-03	1.17E-02	2.10E-05	2.97E-03	4.42E-04
A2-12	3.83E-02	1.72E-04	1.29E-04	2.29E-04	3.49E-04	1.03E-03	1.07E-04	3.59E-03	1.28E-02	1.15E-04	3.52E-03	2.01E-03
A2-13	3.92E-02	2.02E-04	2.17E-06	2.37E-04	5.59E-05	9.81E-04	4.11E-05	3.38E-03	1.14E-02	7.91E-04	4.61E-03	3.13E-04
A2-14	4.04E-02	6.66E-05	2.22E-05	4.79E-04	1.04E-03	1.59E-03	6.39E-04	3.35E-03	1.40E-02	2.06E-04	4.94E-03	6.56E-04
A2-15	3.78E-02	1.18E-04	8.42E-05	4.05E-04	1.84E-04	1.02E-03	2.57E-04	3.05E-03	1.31E-02	6.29E-04	2.90E-03	1.59E-03
A2-16	4.22E-02	1.16E-04	9.49E-05	2.13E-04	8.49E-04	2.62E-03	5.00E-04	3.49E-03	1.49E-02	3.43E-04	4.96E-03	1.38E-03
A2-17	3.48E-02	2.71E-04	1.93E-04	5.04E-04	5.49E-03	1.12E-02	4.84E-04	2.80E-03	2.94E-02	5.04E-04	2.97E-03	7.31E-04
A2-18	3.72E-02	1.50E-04	4.46E-05	3.23E-04	7.89E-04	3.62E-03	3.14E-04	2.24E-03	1.14E-02	5.61E-04	4.79E-03	9.66E-04
A2-19	3.50E-02	4.65E-05	3.03E-05	2.28E-04	1.60E-03	4.97E-02	1.52E-04	2.52E-03	1.62E-02	1.78E-04	4.27E-03	3.07E-03
A3-7	3.29E-02	1.17E-04	2.27E-03	3.12E-05	6.67E-04	5.73E-03	1.72E-04	2.80E-03	1.14E-02	7.94E-05	3.37E-03	3.01E-03
A3-8	3.83E-02	1.14E-04	6.90E-05	6.32E-04	8.65E-04	7.66E-04	3.79E-04	2.67E-03	1.37E-02	7.74E-04	3.68E-03	2.38E-03
A3-9	3.82E-02	1.93E-04	3.87E-05	2.31E-04	1.95E-04	4.18E-03	2.63E-04	3.46E-03	1.32E-02	3.15E-04	4.26E-03	1.63E-03
A3-10	3.98E-02	1.59E-04	1.60E-04	5.09E-04	3.19E-04	3.41E-04	5.67E-04	3.53E-03	1.29E-02	9.19E-04	2.68E-03	1.84E-03
A3-11	3.73E-02	1.02E-04	7.11E-05	3.15E-04	1.59E-04	4.60E-03	3.34E-05	3.27E-03	1.12E-02	9.60E-04	4.32E-03	1.51E-03
A3-12	4.02E-02	2.20E-05	1.66E-04	2.39E-04	2.78E-04	1.56E-04	2.93E-04	2.29E-03	1.12E-02	1.36E-04	3.78E-03	1.34E-03
A3-13	4.13E-02	2.92E-05	3.31E-05	1.51E-04	1.11E-03	4.82E-03	4.77E-04	3.30E-03	2.25E-02	9.46E-05	4.05E-03	3.91E-03
A3-14	3.96E-02	7.63E-05	9.29E-05	2.55E-04	6.25E-04	7.35E-04	2.37E-04	2.67E-03	1.17E-02	8.92E-04	5.07E-03	1.34E-03
A4-1	4.04E-02	1.47E-04	2.50E-05	4.18E-05	4.08E-04	5.77E-04	1.67E-04	2.69E-03	1.12E-02	6.79E-05	5.23E-03	1.16E-03
A4-2	3.64E-02	2.36E-04	2.87E-04	5.66E-04	8.22E-05	4.85E-02	1.60E-04	2.99E-03	1.44E-02	1.09E-03	3.98E-03	5.04E-04
A4-3	3.84E-02	1.21E-04	7.32E-05	1.22E-04	8.08E-04	8.77E-04	2.54E-04	2.56E-03	1.24E-02	3.07E-05	3.32E-03	8.99E-04
A4-4	3.29E-02	1.72E-04	1.37E-04	2.19E-05	1.71E-03	7.94E-02	7.52E-05	1.96E-03	1.66E-02	1.18E-04	2.63E-03	1.18E-03
A4-5	3.71E-02	2.53E-04	7.80E-05	3.49E-05	3.40E-04	1.51E-03	1.53E-04	3.06E-03	1.98E-02	7.38E-04	4.51E-03	9.96E-04
M6	4.08E-02	3.70E-05	2.40E-05	3.17E-04	9.07E-04	2.71E-03	3.44E-04	2.60E-03	1.20E-02	2.13E-04	4.93E-03	2.11E-03
M7	3.78E-02	2.62E-04	2.36E-04	5.83E-04	1.05E-03	1.10E-02	8.53E-04	2.49E-03	3.17E-02	2.75E-04	4.33E-03	3.66E-03
M8	3.56E-02	1.87E-04	2.17E-04	6.84E-04	6.42E-04	2.39E-02	1.19E-03	3.34E-03	2.40E-02	4.91E-04	4.11E-03	1.50E-03
M9	3.61E-02	1.01E-04	1.54E-04	1.01E-03	1.07E-03	3.81E-03	1.93E-03	2.59E-03	6.90E-02	7.47E-04	4.50E-03	1.81E-03
M10	4.07E-02	4.42E-05	6.19E-05	6.57E-04	1.51E-03	2.04E-03	1.05E-03	3.01E-03	2.59E-02	6.32E-04	4.30E-03	2.62E-03
CN1	4.04E-02	8.36E-05	5.77E-05	1.65E-04	4.48E-04	3.90E-04	4.31E-04	3.09E-03	1.11E-02	3.77E-04	4.04E-03	1.95E-03
CN2	3.87E-02	1.79E-04	2.93E-04	1.23E-03	1.71E-03	1.43E-03	3.11E-04	3.04E-03	1.71E-02	8.02E-04	3.73E-03	5.73E-04
CC3-1	3.09E-02	1.17E-03	2.31E-04	5.62E-04	3.03E-03	3.34E-02	8.95E-04	2.15E-03	2.71E-02	7.92E-04	4.05E-03	9.97E-04
CC3-2	3.49E-02	1.61E-04	7.77E-05	1.47E-05	2.07E-03	8.30E-03	2.61E-04	3.07E-03	1.65E-02	2.73E-04	3.46E-03	4.78E-04
CC3-3	3.35E-02	7.88E-04	1.30E-04	5.91E-04	1.28E-03	1.57E-02	8.15E-04	1.96E-03	1.81E-02	7.40E-04	3.36E-03	2.19E-03
CC3-4	3.06E-02	2.41E-03	4.37E-04	3.74E-04	2.78E-03	3.62E-02	2.24E-03	2.40E-03	2.75E-02	1.62E-04	3.24E-03	4.47E-04
UV-1	3.97E-02	8.07E-05	8.35E-05	3.05E-04	5.42E-04	5.52E-03	4.65E-04	3.15E-03	1.28E-02	6.22E-04	3.70E-03	1.30E-03
UV-2	4.08E-02	3.20E-04	1.98E-04	4.06E-04	4.02E-05	9.51E-04	2.05E-04	3.51E-03	8.89E-03	5.28E-04	3.10E-03	2.43E-03
UV-3	3.89E-02	6.52E-05	6.96E-05	3.92E-04	8.37E-05	4.71E-05	7.66E-05	3.30E-03	9.41E-03	1.25E-03	4.19E-03	8.04E-04

Copyright © 2015 John Wiley & Sons, Ltd.

beam diameter in the surface of the sample is about 80 mm^2. These elements were fitted together on a mechanical device that allows us to place the system in front of the analysis point and to maintain the same geometry ensuring the reproducibility of the measurements. The X-ray beam impinges perpendicular to the sample, and a tube and a detector were placed with an excitation-detection geometry of 45° and a 2 cm sample-detector distance. All samples were left untreated except for cleaning with mineralized water prior to the non-destructive EDXRF analysis, with the spectrometer operating at a voltage of 30 kV, a current of 4 μA and an acquisition time of 180 s.

In general, flint is composed by polymorphs of SiO_2. However, their proportion and the presence of impurities such as calcite, iron oxides, organic matter or other compounds make its characteristics and composition variable from area to area of the sample.[17,18] In other words, one of the limitations of the chemical characterization of flint is its heterogeneity. Although EDXRF is a suitable analytical technique to obtain qualitative and/or quantitative data for most elements of the periodic table, these data come from a limited area of the sample defined by the X-ray beam size, and then many measurements are necessary on a same sample. Selected samples were analysed at several discrete locations, and net areas of the fluorescence K lines generated at each location were averaged and normalized to the total count of the spectra (Table 2). Values for reproducibility, expressed as relative standard deviations (RSD), were calculated for major detected elements (Si, K, Ca and Fe) and yield RSD values <15%. In this preliminary study, measurement points were selected on relatively flat areas of each flint sample with no cortex or inclusions, and we have performed the data analysis with the averaged values of these measurements. A comparison is established between the defined groups from macroscopic classification of the samples and the defined groups based on a multivariate classification procedure by means of principal components analysis (PCA) and hierarchical cluster analysis (HCA) on the EDXRF data.

XRD analyses

A selected set of 26 samples (see Table 3) with no archaeological interest was analysed by XRD in order to study the possibility to discriminate between local and allochthonous flint samples. XRD were carried out using a Bruker D8-Advance diffraction system operating at 40 kV and 30 mA with monochromatic Cu–Kα radiation. The samples were powered in an agatha mortar and mounted in conventional aluminium holders prior to the measurements. The intensity was measured in the 2θ range from 5° to 80° at a step size of 0.02° and a counting time of 0.2 s per step. Additionally, XRD patterns were also used to calculate the IC of quartz considering the degree of resolution of the quintuplet at 2θ zone 67°–69° and the intensity of the peak at 2θ = 67.74°.[19,4]

Results and discussion

Examination under stereomicroscope allowed us to identify flint artefacts found in the Abrigo de la Quebrada site and to distinguish reliably between different varieties of flint by employing a combination of several features (translucence, colour, texture, impurities, grain, lustre, characteristics of the cortex and knapping facility). Using these features, five types of flint artefacts were identified among the samples from the Abrigo de la Quebrada site and surrounding quarries: one local type and four allochthonous types.[15]

Table 3. Crystalline phases and index of crystallinity (IC) of archaeological and geological samples

Sample	Origen (macroscopic type)	Crystalline phase	IC
D13	Abrigo de la Quebrada (local)	Quartz, Calcite, Sodium Silicate	2.5
D14	Abrigo de la Quebrada (local)	Quartz, Calcite	1.7
D15	Abrigo de la Quebrada (local)	Quartz, Calcite	2.5
D16	Abrigo de la Quebrada (local)	Quartz, Calcite	1.5
D18	Abrigo de la Quebrada (local)	Quartz, Calcite	1.5
D19	Abrigo de la Quebrada (local)	Quartz, Calcite	2.4
D20	Abrigo de la Quebrada (local)	Quartz	1.1
A1-6	Abrigo de la Quebrada (alloc. type 1)	Quartz, Calcite	1.1
A1-7	Abrigo de la Quebrada (alloc. type 1)	Quartz, Pyrolusite	<1
A2-16	Abrigo de la Quebrada (alloc. type 2)	Quartz, Calcite	<1
A2-17	Abrigo de la Quebrada (alloc. type 2)	Quartz, Calcite, Iron Oxide III	<1
A2-18	Abrigo de la Quebrada (alloc. type 2)	Quartz, Calcite	1.5
A2-19	Abrigo de la Quebrada (alloc. type 2)	Quartz, Calcite	<1
A3-10	Abrigo de la Quebrada (alloc. type 3)	Quartz, Manganese Oxide	<1
A3-12	Abrigo de la Quebrada (alloc. type 3)	Quartz, Moganite, Calcite	<1
A3-13	Abrigo de la Quebrada (alloc. type 3)	Quartz	<1
A3-14	Abrigo de la Quebrada (alloc. type 3)	Quartz, Calcite	<1
CC3-1	Cova de les Cendres	Quartz, Calcite	<1
CC3-2	Cova de les Cendres	Quartz, Calcite	1.5
CC3-3	Cova de les Cendres	Quartz	<1
CC3-4	Cova de les Cendres	Quartz	3.4
M6	Corrales de Silla quarry (local)	Quartz, Calcite	3.2
M7	Collado de las Granzas quarry (local)	Quartz, Calcite	2.8
M8	Barranco Artaj quarry (local)	Quartz, Calcite	3.9
M9	Las Ramblillas quarry (local)	Quartz, Calcite	2.4
M10	CV 35 quarry (local)	Quartz, Calcite	2.4

The local flint type called Domeño-type (samples labelled as D) is the most abundant, and its stratotype is located on the hillsides of the Turia river from 5 to 8 km around the site. This flint occurs in Middle Jurassic formations (between 174.1 and 163.5 millions of years ago) and is of good knapping quality, fine-grained and shiny. Its surface is smooth, without inclusions, opaque and with a microcrystalline texture. The base colour is grey with shades of dark green homogeneously distributed and presents a semi-rugged external appearance. It also occurs as irregular nodules that are incrusted in limestone blocks and present different morphologies (longish, globular, etc.) and a rather thin cortex (Fig. 2). This type has detrital macroquartz mosaics and numerous inclusions. The non-siliceous components show the presence of iron oxides (hematite) and other relict minerals. A silicification process by stages can also be observed, forming a first generation of fibrous quartz and a second generation of macroquartz grains. The concave and convex contacts of this type show the presence of calcium carbonate that has preceded the silicification. The presence of triaxone sponge spicules and microforaminifera indicates a formation in marine environments.

Geological samples from the surrounding quarries located at the vicinity of the Abrigo de la Quebrada site (samples labelled as M) have the same typology and similar properties and macroscopic features as those of the Domeño-type flint artefacts.

The allochthonous flints (samples labelled as A) constitute a group with different macroscopic attributes from the Domeño local type and can be classified into four subgroups (Types 1, 2, 3 and 4;

Copyright © 2015 John Wiley & Sons, Ltd.

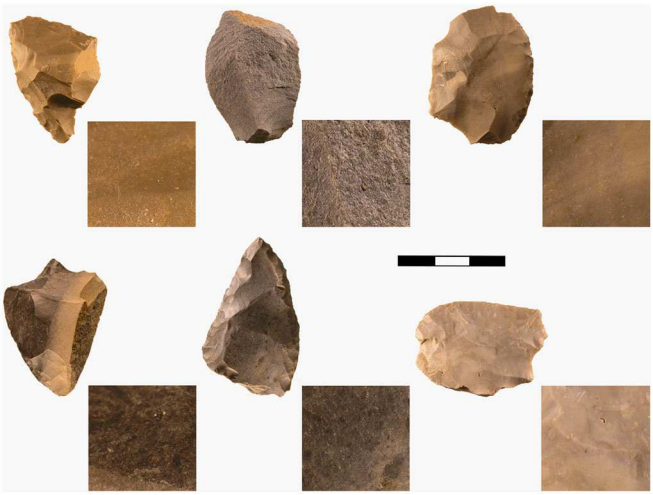

Figure 2. Local, Domeño-type, flint samples from the Abrigo de la Quebrada site (OM, 40×).

see Fig. 3). Type 1 has whitish colour with brownish and yellowish hues. The cortex indicates continental formation in an evaporitic sedimentary basin probably linked to a Tertiary geological formation. This type is fine-grained, translucent and with few intrusions (most is silica). Some inclusions (acicular pseudomorphs gypsum crystals, iron oxide cryptograins and anhydritical components) indicate flint formation environments with high salinity levels. Flint Type 2 is fine-grained, with a smooth surface and microcrystalline structure, and has a good knapping quality. Its colour is light brown with small dark speckles. Internally, spicule sections, inertites and the presence of microforaminifera indicate a marine formation environment, probably of Cretaceous age. An

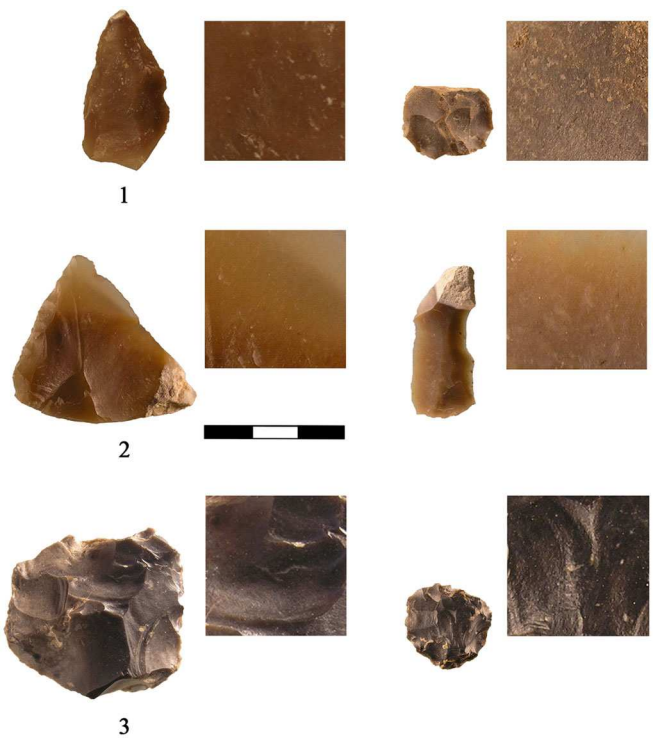

Figure 3. Allochthonous types of flint from the Abrigo de la Quebrada site (OM, 40×).

interesting point is that some artefacts of this type show remains of whitish patinas as well as of a fine smooth cortex; these features suggest that the sources correspond to tabular siliceous formations absent in the geographic area around the site. Type 3 is mainly characterized by its blackish colour. As Type 2, it is also good for knapping, fine-grained with a smooth surface and a microcrystalline structure. The presence of intraclasts of biogenic origin along with algae remains and sea urchin spicules suggests a marine depositional environment for this type. Finally, a fourth type (Type 4) includes flint artefacts that remains incompletely characterized and does not fit into any of the other macroscopic types.

With relation to the foreign samples, the flint artefacts from Cova de les Cendres are characterized by fine-grained microcrystalline texture and good knapping quality. Their colourations are brown, grey and black with small light and dark spots. The presence of microforaminifera, inertites and sponge spicules suggests a marine formation environment. Flint artefacts from the Cova Negra show similar macroscopic characteristics as those of Type 2 local artefacts.

EDXRF measurements were taken with special care to selected flat surfaces on the flint samples and to avoid the analysis of patinated surfaces. Table 2 shows the normalized net areas from the characteristic K-lines of the elements found in the analysed samples: Si, P, S, Cl, K, Ca, Ti, V, Fe, Cu, Zn and Sr; these are a subset of elements for which measurements were available for all the samples. The heterogeneity of the measurements is high, especially in regard to the presence of calcium; net areas of this element show, even on the same sample, extreme variability caused by the fluctuating concentrations of calcium minerals. Figure 4 shows a characteristic EDXRF spectrum related to the sample D16. We can see elements present in the flint sample and several elements coming from the spectrometer that are not present in the sample (Ar from the air, Ag and Ni from the spectrometer). The higher count rates correspond to Si, Ca and Fe, while other elements are present as minor or trace elements.

The compositional data obtained by EDXRF have been submitted to multivariate classification procedures such as PCA and HCA, in order to identify similarities and groupings of the samples and to arrange multivariate data sets to reveal clusters that discriminate between local and allochthonous flint samples. Both procedures were performed taking into account as

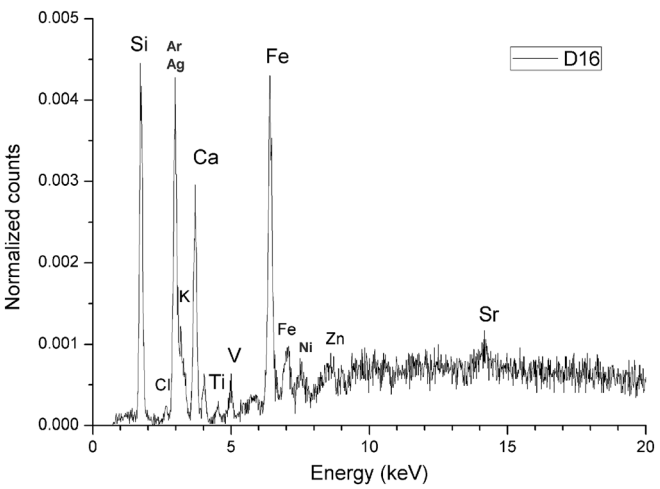

Figure 4. EDXRF spectrum of the flint sample D16.

Copyright © 2015 John Wiley & Sons, Ltd.

variables the net areas of the fluorescence lines normalized to the total counts of the spectra. Multivariate statistical analysis of these data was processed by using the computer software package STATGRAPHICS Centurion (Statpoint Technologies, Inc. Warrenton, VA, USA).

With regard to the PCA, four principal components were extracted covering 79.5% of the cumulative variance. The biplots of the scores for the two first principal components PC1 and PC2 (Fig. 5) show that local samples labelled as D have negative values for PC1 and positive values for PC2; on the contrary, most of the scores of the allochthonous samples have positive values for the principal component PC1. Therefore, it is possible to discriminate between local and allochthonous samples by means of a multivariate analysis. As far as geological samples from the geographical area of Chelva are concerned, four of the five samples (M7, M8, M9 and M10) are projected close to local D samples, while sample M6 is projected together with allochthonous samples due to the presence of low intensity peaks of iron with respect to other quarry samples. This indicates that local samples present similarities with the elemental composition of these regional outcrops and should be the subject of a further detailed study intended to identify the supply sources of local samples. Sample D11 is scored as an outlier and is characterized by calcium and chlorine fluorescence lines higher than the rest of the local samples. On the other hand, the scores of the allochthonous samples do not allow us to make a clear differentiation of the different subsets of samples. The loading plots derived from the first two components (Fig. 5) show that silicon and vanadium are the dominant variables for PC1 positive values, that potassium is the dominant variable for the negative values of the PC1 and that zinc is the dominant variable for the positive values of the PC2 and calcium for the negative values of the PC2. Titanium and chlorine with positive values for the PC2 and negative values for the PC1 are correlated variables. An inverse correlation between silicon and calcium can be observed and can be explained by the presence of calcium compound inclusions.

HCA was considered as the method for exploratory data analysis to arrange multivariate data sets according to their similarity. HCA of this set of data was performed using Ward's method as the

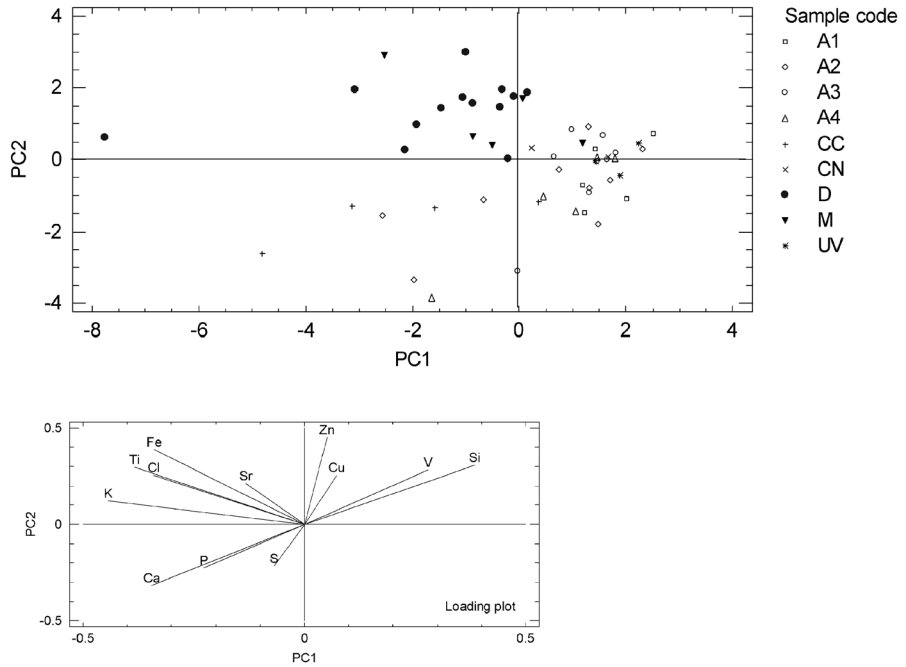

Figure 5. Scatter plot of the scores and loading plot for the first two principal components from EDXRF data.

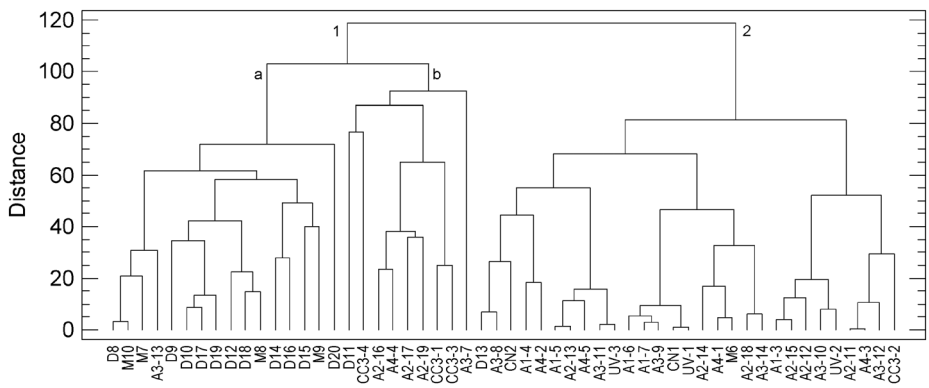

Figure 6. Dendogram resulting from cluster analysis performed on EDXRF data.

Copyright © 2015 John Wiley & Sons, Ltd.

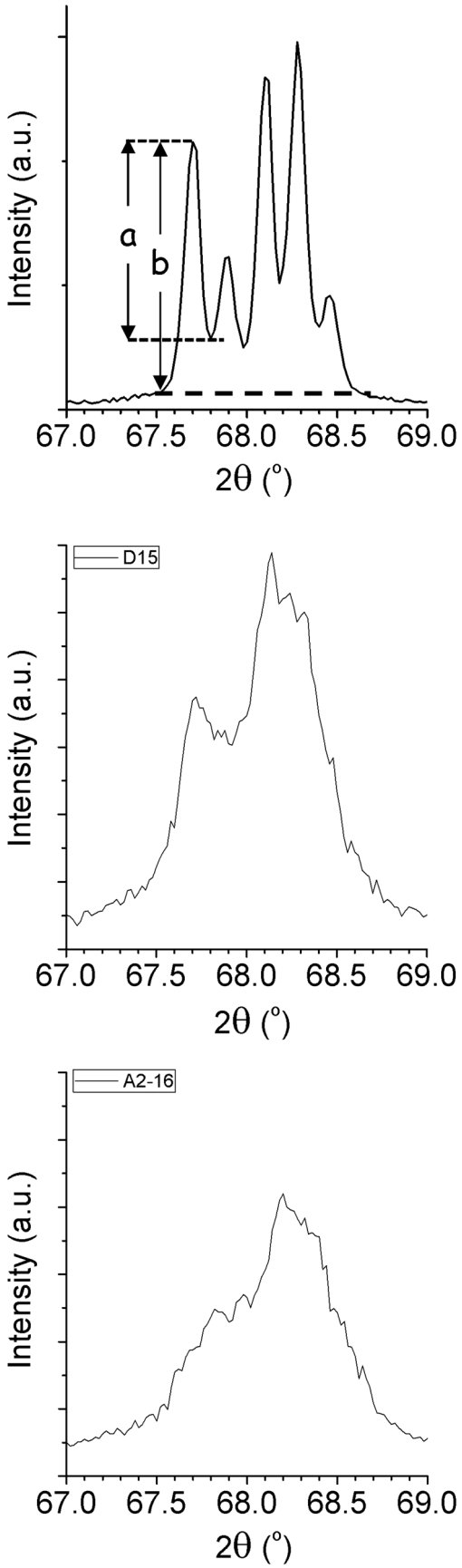

Figure 7. XRD patterns of flint samples with different crystallinity of quartz. Top: euhedral quartz, IC = 10. Centre: sample D15, IC = 2.5. Bottom: sample A2-16, IC < 1.

cluster method with Euclidean distances and transformed values with *z*-scores. Figure 6 shows the dendogram obtained for the detected elements and where we can observe pieces of evidence for the attribution of single cases to two major clusters, one of which included all the local samples except the sample labelled D13 (cluster 1). Inside cluster 1, there is evidence of two subclusters. Subcluster 1a includes local samples and samples from Chelva outcrops whereas subcluster 1b includes the outlier D11 and allochthonous samples with negative scores for the first two principal components PC1 and PC2. The second cluster (cluster 2) is clearly given by macroscopically catalogued allochthonous flint artefacts that are projected together with the foreign flint samples from Alicante (CN1, CN2, UV1 and UV2) and Teruel (UV3). Cluster 2 also includes the macroscopically catalogued sample D13 and the geological sample M6 from the Chelva outcrops, which present similarities in their composition with allochthonous samples. Just as with the PCA, the HCA does not allow us to make a clear differentiation among the different types of allochthonous and foreign samples that are projected in clusters which have no correlation with the macroscopic classification.

Five samples from the outcrops of Chelva and 21 archaeological samples were analysed by XRD (Table 3). The diffractograms show the presence of quartz (SiO_2) as the main crystalline phase, calcite (CO_3Ca) and the occasional presence of pyrolusite (MnO_2), moganite (a polymorph of quartz), silicates and oxides. Comparison between XRD spectra is made difficult due to the dominance of quartz in all of them. Table 3 reports these crystalline phases ordered in relation to the intensity of the diffractogram patterns. XRD diffractograms were also used to calculate the IC of the quartz present in the samples by means of the expression $IC = 10\,F\,a/b$, where a is the height of the 67.79° peak, b is total height above the background (see Fig. 7) and F is a correction factor to express the IC on a standard scale of <1 to 10.[19] This factor was obtained from an XRD pattern of reference well-crystallized euhedral quartz. A value of $F = 1.325$ was used as the correction factor applied to the data. The IC of the archaeological and geological samples presented in Table 3 was generally low according to the scale of Murata and Norman.[19] The crystallinity of Domeño-type flints ranges from 1.1 to 2.5, whereas the crystallinity of flints from Chelva outcrops (samples M6 to M10 in Table 3) ranges from 2.4 to 3.9, which are significantly higher than the crystallinity of the Domeño-type archaeological samples. However, the crystallinity of this set of samples is relatively high in comparison with the poor crystallinity of most allochthonous samples. The 67.74° diffraction peak is barely seen or does not appear at all in 10 of the 14 allochthonous samples with an IC of <1 (Table 3). Figure 7 shows the XRD profiles of 68° quintuplet for well-crystallized euhedral quartz (IC = 10), for the local sample D15 (IC = 2.5) and for poorly crystallized quartz of the allochthonous sample A2-16 (IC < 1). This study supports the separateness of the Domeño-type samples indicated by the multivariate analysis of the EDXRF data, despite the fact that sample M6 is projected together with allochthonous samples but with a higher IC.

Conclusions

Flint artefacts from the Abrigo de la Quebrada site were characterized on the basis of a set of macroscopic observable attributes and catalogued into local flints (Domeño-type flints) and allochthonous flints. Non-destructive EDXRF spectrometry applied to the identification of chemical elements present in archaeological and

Copyright © 2015 John Wiley & Sons, Ltd.

geological flint samples has proved to be adequate to characterize them. Multivariate statistical analysis of the elemental chemical data from portable EDXRF instrumentation has allowed us to discriminate between local and allochthonous flint artefacts in accordance with macroscopic classification. Geological flint samples from the Chelva outcrops in proximity to the Abrigo de la Quebrada site are clustered together with local flint artefacts (Domeño type), while foreign flint samples from outcrops of Alicante and Teruel are clearly differentiated from local samples. However, from the multivariate analysis of the EDXRF data, it is not possible to identify clusters among the allochthonous samples.

XRD analyses of the selected samples show the presence of quartz as the dominant crystalline phase with traces of other minerals, mainly calcite. The obtained results show that the IC, calculated from the Murata and Norman equation, is an appropriate variable to discriminate between local and allochthonous or foreign flint samples. In this sense, local samples (Domeño type labelled as D) and geological samples from the Chelva outcrops (labelled as M) have ICs greater than the allochthonous samples.

The methods used and the results presented in this work supply the basis to define future protocols for sourcing flint artefacts from the Abrigo de la Quebrada site using non-destructive analytical techniques. Our study is still in an initial stage, and the results obtained so far are preliminary and in need of corroboration and augmentation by additional analysis and fieldwork. The planned work includes extended survey to locate as yet unknown sources and the analysis of more samples from a wider range of sites from different parts of the region and from different periods of its prehistory.

Acknowledgements

This project was developed with funds of the research project PROMETEOII/2013/016 from the Generalitat Valenciana and the research projects FFI 2008-01200/FISO, HAR 2008-04273-E/HIST and HAR2011-24878 from the Ministerio de Ciencia e Innovación.

References

[1] N. Malyk-Selivanova, G. M. Ashley, R. Gal, M. D. Glascock, H. Neff. *Geoarchaeology* **1998**, *13*(7), 673–708.
[2] A. Costopoulos. *Fennoscandia Archaeologica XX* **2003**, 41–54.
[3] P. Allard, F. Bostyn, F. Gilignay, J. Lech (Eds), *Flint mining in prehistoric Europe: interpreting the archaeological records*. British Archaeological Reports International Series, vol. *1891*, Archaeopress, Oxford, **2008**.
[4] M. A. Bustillo, M. Castañeda, M. Capaote, S. Consuegra, C. Criado, P. Díaz-del-Río, T. Orozco, J. L. Pérez-Giménez, X. Terradas. *Archaeometry* **2009**, *51*(2), 175–196.
[5] R. E. Hughes, A. Högberg, D. Olausson. *J. Nordic Archaeological Sci.* **2010**, *17*, 15–25.
[6] M. S. Shackley, *X-ray fluorescence spectrometry (XRF) in geoarchaeology*, Springer, New York, **2011**.
[7] R. E. Hughes, A. Högberg, D. Olausson. *Archaeometry* **2012**, *54*(5), 779–795.
[8] G. Gauthier, A. L. Burke, M. Leclerc. *J. Archaeol. Sci.* **2012**, *39*, 2436–2451.
[9] A. García-Carrillo, C. Cacho, S. Ripoll. *Espac. Tiempo Forma. Prehis. Arqueol.* **1991**, *4*, 15–36.
[10] J. Menargues, in *Geoarqueología y Patrimonio en la Península Ibérica y el entorno mediterráneo* (Eds: M. Santonja, A. Pérez-González, M. J. Machado), Adema Patrimonio. Editorial Almazán, Soria, **2005**, pp. 413–424.
[11] E. Faus. *Alberri* **2009**, *19*, 9–38.
[12] F. J. Molina, A. Tarriño, B. Galván, C. Hernández. *Recerques. Mus. Alcoi* **2010**, *19*, 65–80.
[13] M. Tiffagom, *De la Pierre à l'Homme. Essai sur une paléoanthropologie solutréenne, Eraul*, Université de Liège, Service de Prehistoire, Liège, **2006**.
[14] A. Moriel. *Cuad. Prehist. Arqueol. Castellonenses* **1985**, *11*, 17–86.
[15] A. Eixea, V. Villaverde, J. Zilhão. *Trab. Prehist.* **2011**, *68*(1), 65–78.
[16] C. Roldán, V. Villaverde, I. Ródenas, F. Novelli, S. Murcia. *J. Archaeol. Sci.* **2013**, *40*, 744–754.
[17] B. E. Luedtke. *Am. Antiquity* **1979**, *44*, 744–757.
[18] M. Olivares, A. Tarriño, X. Murelaga, J. L. Baceta, K. Castro, N. Etxebarria. *Spectrochim. Acta, Part A* **2009**, *73*, 492–497.
[19] K. J. Murata, M. B. Norman. *Am. J. Sci.* **1976**, *276*, 1120–1130.

Copyright © 2015 John Wiley & Sons, Ltd.